Cement and Concrete Research 40 (2010) 984–996

Contents lists available at ScienceDirect

Cement and Concrete Research

journal homepage: http://ees.elsevier.com/CEMCON/default.asp

Modeling the hydration of concrete incorporating fly ash or slag

Xiao-Yong Wang, Han-Seung Lee *

School of Architecture & Architectural Engineering, Hanyang University, Ansan, 425-791, Republic of Korea

ARTICLE INFO

Article history:
Received 15 July 2009
Accepted 1 March 2010

Keywords:
Granulated blast-furnace slag (D)
Fly ash (D)
Hydration (A)
Modeling (E)
High-performance concrete (E)

ABSTRACT

Granulated slag from metal industries and fly ash from the combustion of coal are industrial by-products that have been widely used as mineral admixtures in normal and high strength concrete. Due to the reaction between calcium hydroxide and fly ash or slag, the hydration of concrete containing fly ash or slag is much more complex compared with that of Portland cement. In this paper, the production of calcium hydroxide in cement hydration and its consumption in the reaction of mineral admixtures is considered in order to develop a numerical model that simulates the hydration of concrete containing fly ash or slag. The heat evolution rates of fly ash- or slag-blended concrete is determined by the contribution of both cement hydration and the reaction of the mineral admixtures. The proposed model is verified through experimental data on concrete with different water-to-cement ratios and mineral admixture substitution ratios.

1. Introduction

Both granulated slag and fly ash are general industrial by-products that have long been used as mineral admixtures to improve durability and produce high strength and high performance concrete. In addition, economic and ecological benefits, such as energy-savings and resource-conservation, can be achieved using blended cement [1,2].

The hydration of cement is an exothermic process generating a considerable amount of heat. The relatively low thermal conductivity of concrete causes a sharp temperature gradient near the surface and a high temperature in the cores of massive structures early in their construction. This may lead to thermal stress and undesirable thermal cracking if external or internal restraints exist. A cogent simulation of an exothermic hydration process in cement plays a crucial role in quantifying thermal stress and assessing the risk of thermal cracking in mass concrete structures. Tomosawa [3] proposed a hydration model to estimate the heat liberation rate during the hydration of Portland cement and the adiabatic temperature rise in concrete. In this model, the residual concentration of water is used as a parameter indicating the decline of reaction rate toward the reaction end point. The influence of temperature on cement hydration is considered by Arrhenius's law. Based on Tomosawa's model, Park [4,5] constructed a microstructural hydration model of Portland cement that considers the reduction in the hydration rate that occurs due to the reduction of free water and the reduction of the interfacial area of contact between the free water and the hydration products. Based on a hydration model using a finite element method, the temperature distribution of high strength concrete was evaluated. Swaddiwudhipong [6] proposed a multi-constituent model of Portland cement hydration by combining Maekawa's multi-component model [7] with Parrot's hydration model [8]. The concept of equivalent maturity is introduced explicitly to reflect the influence of temperature on the rate of hydration heat release.

Compared with Portland cement, the hydration of cement incorporating supplementary cementing materials (SCM), such as fly ash, slag, or silica fume, is much more complex due to the coexistence of cement hydration and the reactions of the mineral admixtures. Swaddiwudhipong [9] presented a hydration model to estimate the heat release of mass concrete in the presence of silica fume. In the model, the degree of reaction of silica fume is evaluated through the degree of cement hydration. The model is valid when the amount of silica fume is limited to less than 10% of the weight of the cement. Maekawa [10–12] proposed a general hydration model (DuCOM) for concrete incorporating fly ash and slag. Fly ash and slag reactions are treated separately from those of ordinary Portland cement, and some interactions are taken into account through the free water content and the calcium hydroxide concentration. Considering the exothermic characteristic and the reaction ratio of slag, Tanaka [13] suggested a method to estimate the adiabatic temperature rise in slag-blended concrete. Schutter [14,15] proposed a kinetic hydration model valid both for Portland cement and blast furnace slag cement. In Schutter's model, the heat evolution of blast furnace slag cement is obtained by the superposition of the heat productions of the Portland reaction (P reaction) and the slag reaction (S reaction). The evolution of mechanical properties in early-age concrete is described using functions of the degree of hydration.

As shown in Refs. [10–15], it is typical to consider the hydration reactions of cement and the blended mineral admixtures to model the hydration of blended concrete. In this paper, a numerical model is

* Corresponding author. Tel./fax: +82 31 400 5181.
E-mail address: ercleehs@hanyang.ac.kr (H.-S. Lee).

0008-8846/$ – see front matter © 2010 Elsevier Ltd. All rights reserved.
doi:10.1016/j.cemconres.2010.03.001

proposed to simulate the hydration of concrete containing fly ash and slag. By considering the production of calcium hydroxide in cement hydration and its consumption during the reactions of the mineral admixtures, the reaction of fly ash and slag is separated from that of cement hydration. The heat evolution rate of blended concrete is determined by the contributions of both the cement hydration and the reactions of the mineral admixtures. The temperature rise in concrete containing mineral admixtures may also be evaluated based on the degrees of hydration of the cement and the mineral admixtures.

2. Hydration model of Portland cement

2.1. Hydration mechanism

In this hydration model, the influences of the water-to-cement ratio, cement particle size distribution, cement mineral components, and curing temperature on the hydration reaction of Portland cement are considered. At the beginning of the hydration simulation, cement particles are randomly cast into the representative unit cell space, as shown in Fig. 1. It is assumed that cement hydration will start when cement and water come into contact, and the hydrate formed by the hydration adheres spherically to the cement particles.

The basic hydration equation is described in Eq. (1), which was developed by Tomosawa [3] to describe the hydration of a single cement particle. His model consists of a single equation composed of four rate determining coefficients, which consider the rates of formation and destruction of an initial impermeable layer, the activated chemical reaction process and the following diffusion-controlled process.

$$\frac{d\alpha^j}{dt} = \frac{3C_{w\infty}}{\left(v + w_{ag}\right)r_0^j\rho}\frac{1}{\left(\frac{1}{k_d} - \frac{r_0^j}{D_e}\right) + \frac{r_0^j}{D_e}\left(1-\alpha^j\right)^{\frac{-1}{3}} + \frac{1}{k_r}\left(1-\alpha^j\right)^{\frac{-2}{3}}} \tag{1}$$

In the equation above, α^j denotes the degree of hydration of cement particles; j refers to an individual cement particle; v is the stoichiometric ratio of the masses of water to cement; w_{ag} is the physically bound water; ρ is the density of cement; r_0^j is the radius of anhydrate cement particles; D_e is the effective diffusion coefficient of water in the hydration product; $C_{w\infty}$ is the concentration of water at the outer region of the gel; k_r is the coefficient of the reaction rate of cement; and k_d is the reaction coefficient in a dormant period that is assumed to be a function of the hydration degree during the initial reaction period, as expressed in Eq. (2):

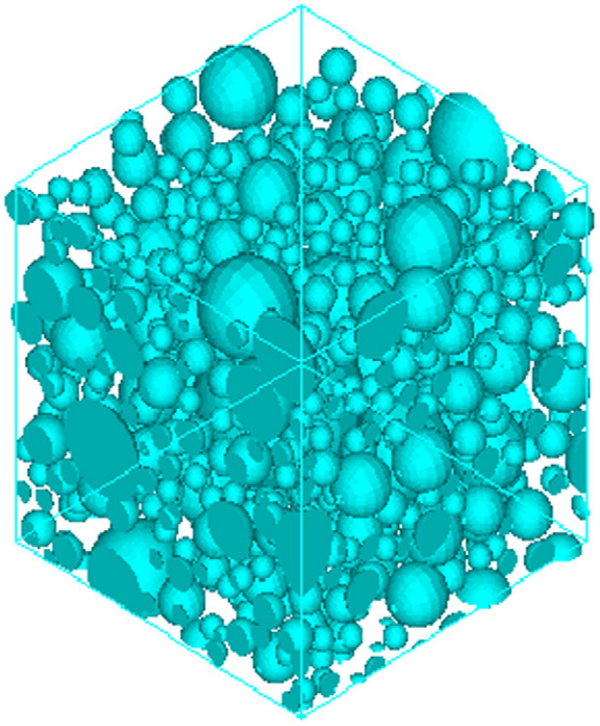

Fig. 1. Cement particles distribute randomly in cell space.

$$k_d = \frac{B}{\left(\alpha^j\right)^{1.5}} + C\left(r_0^j - r_t^j\right)^4 \tag{2}$$

where B and C are the rate determining coefficients of cement hydration and r_t^j is the inner radius of the hydrating cement particle.

The effective diffusion coefficient of water is affected by the tortuosity of the gel pores as well as the radii of the gel pores in the hydrate. This phenomenon can be described as a function of the degree of hydration and is expressed by Eq. (3):

$$D_e = D_{e0}\ln\left(\frac{1}{\alpha^j}\right) \tag{3}$$

where D_{e0} is the initial diffusion coefficient.

The influence of temperature on cement hydration is considered by the Arrhenius law [3] in Eqs. (4)–(6):

$$B = B_{20}\exp\left(-\beta_1\left(\frac{1}{T} - \frac{1}{293}\right)\right) \tag{4}$$

$$D_e = D_{e20}\exp\left(-\beta_2\left(\frac{1}{T} - \frac{1}{293}\right)\right) \tag{5}$$

$$k_r = k_{r20}\exp\left(-\frac{E}{R}\left(\frac{1}{T} - \frac{1}{293}\right)\right) \tag{6}$$

where B_{20}, D_{e20}, and k_{r20} are the values of B, D_e, and k_r at 293 K, respectively, and β_1, β_2, and E/R are the activation energies of B, D_e, and k_r respectively. The activation energies can be determined from the cement hydration experiments performed at different curing temperatures [3].

When cement is mixed with water, its hydration proceeds according to the model described in the previous section. The degree of hydration of cement can be calculated as follows:

$$\alpha = \sum_{j=1}^{j=n}\alpha^j g^j \tag{7}$$

where g^j is the weight fraction of the individual particle j and n is the total number of cement particles in the cell space. As shown in Eq. (7), the global degree of cement hydration is the average of the hydration degrees of the individual cement particles.

2.2. Water withdrawal mechanism

During the hydration period, at a certain point after the initial setting time, the contact area between the cement particles and the surrounding water will decrease due to the increase in interconnections among the cement particles. As a result, a slower hydration rate will be achieved.

Water present in the paste can be classified into evaporable and non-evaporable fractions. The former consists of capillary water and gel water that resides partially within the hydration product. The non-evaporable water is defined as bound water that chemically reacts with cement. During the hydration process, only the capillary water contributes to further hydration. As the hydration process proceeds, due to the consumption of capillary water and the relative stage of reactivity of the various cement compounds, the relative hydration

rate will decrease. Under conditions of sealed-curing, when the water-to-cement ratio is less than 0.42, due to a limited amount of available water, cement hydration is not complete [3].

By considering these two points, Eq. (1) can be modified to form Eqs. (8-1) and (8-2) [4,16]:

$$\left(\frac{d\alpha^j}{dt}\right)' = \frac{d\alpha^j}{dt} * \left(\frac{freesurface}{totalsurface}\right)^j * \frac{w_{cap}}{w_0} \quad (8-1)$$

$$w_{cap} = w_0 - 0.42 * Ce_0 * \alpha \quad (8-2)$$

where $\left(\frac{freesurface}{totalsurface}\right)^j$ is the ratio between the free surface area (the area which contacts water) and the total surface area that is determined by Navi's proposed method [17]; w_{cap} is the mass of the capillary water; w_0 is the total water mass; Ce_0 is the cement mass in a mixing proportion, and $\frac{w_0 - 0.42 * Ce_0 * \alpha}{w_0}$ describes the decrease in the capillary water available for cement hydration.

3. Hydration model for cement blended with fly ash or slag

3.1. Amount of calcium hydroxide (CH) during the hydration process

As proposed by Papadakis [18–22], during the hydration period, the chemical reactions of the mineral components of Portland cement can be expressed by Eqs. (9-1), (9-2), (9-3), and (9-4):

$$2C_3S + 6H \rightarrow C_3S_2H_3 + 3CH \quad (9-1)$$

$$2C_2S + 4H \rightarrow C_3S_2H_3 + CH \quad (9-2)$$

$$C_3A + C\bar{S}H_2 + 10H \rightarrow C_4A\bar{S}H_{12} \quad (9-3)$$

$$C_4AF + 2CH + 10H \rightarrow C_6AFH_{12} \quad (9-4)$$

Eqs. (9-1), (9-2), (9-3) and (9-4) can be used to determine the amounts of calcium hydroxide and chemically bound water according to the mineral composition of Portland cement [18–22]. Using Eqs. (9-1) to (9-4), it can be shown that when 1 g of cement is hydrated, approximately 0.25 g of chemically bound water will be produced (according to Eqs. (9-1) to (9-4), when 1 g C_3S, C_2S, C_3A and C_4AF hydrates, 0.236 g, 0.209 g, 0.666 g and 0.37 g chemically bound water is necessary respectively.). It should be noted that the amount of physically bound water is not included in Eqs. (9-1) to (9-4). In this paper, it is assumed that when 1 g of cement is hydrated, the sum of chemically bound water and physically bound water equals 0.42 g, as shown in Eqs. (8-1) and (8-2).

Based on the experimental investigation of the amount of calcium hydroxide and the degree of hydration of cement, Sakei [23] and Pane [24] reported that during the hydration of cement paste, the amount of calcium hydroxide is directly proportional to the degree of hydration of cement. Hence, by combining Papadakis' chemical equation with the degree of hydration of cement, the mass of calcium hydroxide in a unit volume of concrete can be obtained with Eq. (10):

$$CH = (0.49 * g_{c3s} + 0.22 * g_{c2s} - 0.3 * g_{c4af}) * Ce_0 * \alpha \quad (10)$$

where g_{c3s}, g_{c2s}, and g_{c4af} are the weight fractions of the mineral components C_3S, C_2S, and C_4AF, respectively.

Fly ash is a pozzolanic material that primarily consists of siliceous and aluminous phases and, in itself, possesses no or few cementing properties but will, in a finely divided form and in the presence of moisture, chemically react with calcium hydroxide to form compounds possessing cementitious properties. Compared with fly ash, slag is self-cementing. It does not require calcium hydroxide to form cementitious products. However, when slag hydrates by itself, the amount of cementitious products formed and the rates of formation are insufficient for use in structural applications. When used in combination with Portland cement, the hydration of slag is accelerated due to the presence of calcium hydroxide [1].

Maekawa [10–12] made a systematic investigation of hydration, microstructural formation, and mass transport of Portland cement concrete and blended concrete. Based on analysis of the experimental results of the amount of chemically bound water, adiabatic temperature rise, and temperature measurement of small quasi-adiabatic blocks, Maekawa said that the reaction of slag and fly ash can be roughly described by the following approximate key figures:

1) The chemical reaction of slag:

Chemically bound water	0.30 g/g slag
Gel water	0.15 g/g slag
Calcium hydroxide	0.22 g/g slag
Total heat generation	110 kcal/kg slag

2) The pozzolanic reaction of fly ash:

Chemically bound water	0.10 g/g fly ash
Gel water	0.15 g/g fly ash
Calcium hydroxide	1.00 g/g fly ash
Total heat generation	50 kcal/kg fly ash.

Using the hydration model and the stoichiometry of the fly ash and slag reaction proposed by Maekawa [10–12], the amounts of calcium hydroxide, chemically bound water, and capillary water in cement–fly ash blends and cement–slag blends during hydration can be determined with the following equations:

$$CH = (0.49 * g_{c3s} + 0.22 * g_{c2s} - 0.3 * g_{c4af}) * Ce_0 * \alpha - RCH_{FS} * \alpha_{FS} * P \quad (11-1)$$

$$w_{cap} = w_0 - 0.42 * Ce_0 * \alpha - RCW_{FS} * \alpha_{FS} * P - RPW_{FS} * \alpha_{FS} * P \quad (11-2)$$

$$w_{cbm} = 0.23 * Ce_0 * \alpha + RCW_{FS} * \alpha_{FS} * P. \quad (11-3)$$

In Eqs. (11-1), (11-2) and (11-3), CH, w_{cap}, and w_{cbm} are the masses of calcium hydroxide, capillary water, and chemically bound water, respectively; α_{FS} is the ratio between the released heat and the total heat generation of the fly ash or slag; P is the mass of the fly ash or slag in the mixture proportion; RCH_{FS} is the mass of reacted calcium hydroxide in the reaction of fly ash or slag; RCW_{FS} is the mass of chemically bound water in the reaction of fly ash or slag; and RPW_{FS} is the mass of gel water in the reaction of fly ash or slag. As shown in Eq. (11-1), the evolution of the mass of calcium hydroxide is dependent on two factors, the production of calcium hydroxide from the hydration of Portland cement and its consumption by the chemical activity of the mineral admixtures. As shown in Eq. (11-2), capillary water is consumed by both the cement hydration and the reaction of the mineral admixtures. As shown in Eq. (11-3), both the hydration of Portland cement and the reaction of mineral admixtures contribute to chemically bound water.

3.2. Simulation of the hydration reaction in cement–slag and cement–fly ash blends

The proposed model is based on the similarity of the mechanisms of cement hydration and of the reaction of mineral admixtures. First, the cement reacts with water, and the glass phase of the mineral admixture reacts with calcium hydroxide. The cement hydration process includes an initial dormant period, a phase-boundary reaction

period, and a diffusion period. In the late stage of cement hydration, diffusion is a control process. Some researchers have reported the reaction of mineral admixtures was a diffusion-controlled process [25–27]. Based on the analysis of the SEM micrographs of Portland cement paste, slag–cement paste, and fly ash–cement paste, Papadakis [18–22] and J.I. Escalante [28,29] reported that the cement hydration product adheres to the surface of unreacted cement particles and the reaction product of mineral admixtures adheres to the surface of unreacted mineral admixture particles. Small cement particles have a high reactivity to water and show little initial dormancy, while larger cement particles show an initial dormant period [4]. Similarly, silica fume is a highly pozzolanic cement replacement material that shows almost no initial dormant period, much like small cement particles [18]. Fly ash shows a long initial dormant period. On the other hand, the hydration rate of mineral admixtures depends on the relative stage of reactivity and the amount of calcium hydroxide in the hydrating blends [23,30,31]. We deduce an equation from cement hydration for the reaction of mineral admixtures by considering both the similarity and the difference between the two reactions.

In the simulation, it is assumed that the reaction of mineral admixtures is divided into three processes: an initial dormant period, a phase-boundary reaction and diffusion processes. By considering these points and using the method proposed by Saeki [23], the hydration equations for fly ash or slag can be written as Eqs. (12-1), (12-2) and (12-3):

$$\frac{d\alpha_{FS}}{dt} = \frac{m_{CH}(t)}{P}\left[\frac{w_{cap}}{w_0}\right]_{SL}\frac{3}{v_{FS}r_{FS0}\rho_{FS}}\frac{1}{\left(\frac{1}{k_{dFS}}-\frac{r_{FS0}}{D_{eFS}}\right)+\frac{r_{FS0}}{D_{eFS}}(1-\alpha_{FS})^{-\frac{1}{3}}+\frac{1}{k_{rFS}}(1-\alpha_{FS})^{-\frac{2}{3}}} \quad (12-1)$$

$$k_{dFS} = \frac{B_{FS}}{(\alpha_{FS})^{1.5}} + C_{FS}*(r_{FS0}-r_{FSt})^4 \quad (12-2)$$

$$D_{eFS} = D_{eFS0}*\ln\left(\frac{1}{\alpha_{FS}}\right) \quad (12-3)$$

where $m_{CH}(t)$ is the calcium hydroxide mass in a unit volume of hydrating cement–fly ash or cement–slag blends and can be obtained from Eq. (11-1); P is the fly ash mass or slag mass in the mixing proportion; v_{FS} is the stoichiometric ratio of the mass of CH to fly ash or CH to slag; r_{FS0} is the radius of the fly ash particle or slag particle; ρ_{FS} is the density of the fly ash or slag; k_{dFS} is the reaction rate coefficient in the dormant period (B_{FS} and C_{FS} are coefficients); D_{eFS0} is the initial diffusion coefficient, and k_{rFS} is the reaction rate coefficient. In Eq. (12-1), $\left[\frac{w_{cap}}{w_0}\right]_{SL}$ models the decrease in available capillary water for the reaction of slag. In the case of cement–fly ash blends, this term is not included.

The influence of temperature on hydration is considered by the Arrhenius law as follows:

$$B_{FS} = B_{FS20}\exp\left(-\beta_{1FS}\left(\frac{1}{T}-\frac{1}{293}\right)\right) \quad (12-4)$$

$$D_{eFS0} = D_{eFS20}\exp\left(-\beta_{3FS}\left(\frac{1}{T}-\frac{1}{293}\right)\right) \quad (12-5)$$

$$k_{rFS} = k_{rFS20}\exp\left(-\frac{E_{FS}}{R}\left(\frac{1}{T}-\frac{1}{293}\right)\right) \quad (12-6)$$

where B_{FS20}, D_{eFS20}, and k_{rFS20} are the values of B_{FS}, D_{eFS}, and k_{rFS} at 293 K, respectively, and β_{1FS},β_{3FS}, and E_{FS}/R are the reduced activation energies of B_{FS}, D_{eFS}, and k_{rFS}, respectively. The calibration of parameters will be introduced in Section 4.

The released heat of the hydrating blends consists of contributions from two parts: the released heat from Portland cement hydration and the released heat from the mineral admixture reaction. The total released heat is expressed by Eq. (13):

$$\frac{dQ}{dt} = Ce_0*\sum g_i H_i\frac{d\alpha}{dt} + P*H_{FS}*\frac{d\alpha_{FS}}{dt} \quad (13)$$

where the first term comes from the hydration of Portland cement and the second comes from the reaction of fly ash or slag; H_i is the total heat generation of the individual components of the cement [31,32]; and H_{FS} is the total heat generation content of the fly ash or slag (by comparing the analytical with the experimental data, Maekawa [10] set the total heat generations of slag and fly ash as 110 kcal/kg and 50 kcal/kg, respectively).

As proposed by Gutteridge [33,34] and Lawrence [35–38], the addition of mineral admixtures represents the dilution, physical, and chemical effects on cement hydration.

First, the dilution effect is a consequence of the replacement of cement by the same quantity of a mineral admixture. An increase in the amount of mineral admixtures involves a decrease in the amount of cement and consequently an increase in the water/cement ratio. This dilution effect is considered by the cement hydration model in Eqs. (8-1) and (8-2).

Second, the physical effects include a retardation effect and heterogeneous nucleation. As reported by Lawrence [35–38], the addition of fly ash can retard the hydration of the cement in early age. This retardation could be due to aluminate ions or organic matter dissolved from the fly ash into the aqueous phase which delays the nucleation and crystallization of $Ca(OH)_2$ and CSH. The delay, however, can be partly compensated for by heterogeneous nucleation. The fly ash particles can serve as nucleation sites for the cement particles and promote chemical activation of the hydration process. In the case of cement–slag blends, as proposed by Paine [39], the influences of delay and acceleration effects on the heat evolution of cement are not significant and for practical purposes can be ignored. In this paper, the physical effect of the addition of fly ash on cement hydration is considered through the coefficient B_{20}, which is related to the initial dormant period of cement hydration and is adjusted to fit the experimental results of the temperature rise history, while all other coefficients are not changed. The physical effect of the addition of slag on cement hydration is not considered.

The chemical effect is a sort of chemical activity in the mineral admixtures. The chemical effect is considered in Eqs. (12-1), (12-2), (12-3), (12-4), (12-5), and (12-6), which takes into account the dependence of the chemical activity on the amount of calcium hydroxide and the kinetic reaction mechanisms involved in the reaction of the mineral admixtures.

Because the dilution, physical and chemical effects are all considered, the proposed numerical model can simulate the hydration of concrete containing fly ash or slag. Furthermore, the temperature rise in concrete containing mineral admixtures can be evaluated based on the degree of hydration of cement and the mineral admixtures [40,41].

4. Prediction of the adiabatic temperature rise history and chemically bound water of concrete containing fly ash or slag

The hydration of cement is a highly nonlinear system with complex interactions. To validate the proposed model, multiple checks, including not only the early-stage temperature rise but also the evolution of chemically bound water, are carried out for verification [10,12]. The specimens employed in an adiabatic temperature test are concrete, and the specimens employed in a chemically bound water test are cement paste. The mineral compositions of ordinary Portland cement (OPC1) and moderate-heat

Table 1
The mineral compositions of OPC and MPC.

	Mineral composition (mass %)					Blaine (cm^2/g)
	C_3S	C_2S	C_3A	C_4AF	$C\bar{S}_2H$	
OPC	47.2	27.0	10.4	9.4	3.9	3380
MPC	44.4	33.7	3.7	12.5	3.9	3040

Table 2
The chemical compositions of slag and fly ash.

	Chemical composition (mass %)						Blaine (cm^2/g)
	SiO_2	Al_2O_3	Fe_2O_3	CaO	MgO	SO_3	
Slag	33.4	15.0	0.5	43.1	6.6	0.0	4250
Fly ash	49.5	31.8	4.7	5.6	1.8	0.0	3400

Portland cement (MPC) are shown in Table 1. The chemical compositions of slag and fly ash are shown in Table 2. The influences of casting temperature, water-to-binder ratio, and the mineral admixture replacement ratio on hydration are investigated by an experiment program with conditions analogous to conditions at construction sites.

The mixing proportions of the specimens are shown in Table 3. Three unit binder contents, 200 kg/m^3, 300 kg/m^3, and 400 kg/m^3 were examined for the Portland cement, fly ash blended cement, and slag-blended cement in the adiabatic temperature rise experiments (OPC200, OPC300, OPC400, SG200, SG300, SG400, SG60, SG70, SG80, FA200, FA300, FA400, FA15, FA30, and FA45). The water-to-binder ratio of the specimens varies between 0.4 and 0.785, the slag replacement ratio between 40% and 80%, and the fly ash replacement ratio between 20% and 40%. As described before, the effects of a low water-to-cement ratio on the heat of hydration generation were considered in this study. For the unit cement weight of 400 kg, the water-to-cement ratio is around 40%. It is well known that at least 40% cement weight of water is required for complete hydration of ordinary Portland cement. When the experiments on adiabatic temperature rise are carried out, three casting temperatures 10 °C, 20 °C and 30 °C are examined.

In a series of experiments on chemically combined water, the water-to-binder ratio of the specimens by weight was 0.3, which is a typical power-rich high performance concrete used at sites. Using a low water-to-binder ratio also meant enhancing the sensitivities of the hydration reactions to the amounts of available water. When experiments on chemically bound water were carried out, the specimens were sealed and cured at a constant temperature of 20 °C. The amounts of chemically bound water were measured by performing differential TGA. The specimens were broken at certain intervals after casting, and samples of about 15 mg to 20 mg were taken for TGA. The loss of weight in the sample from 105 °C to 800 °C was interpreted to be the loss of chemically combined water, and suitable corrections were made to take into account the weight loss due to oxidation of unhydrated cement mineral compounds.

Based on the hydration model, the incremental temperature rise in one time step under adiabatic conditions can be calculated as in Eq. (14):

$$\Delta T = \frac{dQ(t)}{Cp(t)} \tag{14}$$

where ΔT is the incremental temperature in one time step; $dQ(t)$ is the released heat that can be determined from Eq. (13); and $Cp(t)$ is the heat capacity of the hydrating concrete that can be calculated as the sum of the individual components of the concrete (the heat capacities of cement, fly ash, slag, sand, aggregate, water, and chemically bound water are 0.84 J/g°C, 0.84 J/g°C, 0.84 J/g°C, 0.9 J/g°C, 0.9 J/g°C, 4.18 J/g°C, and 2.2 J/g°C respectively [4,5]).

The flow chart for a numerical simulation process is shown in Fig. 2. Coefficients in the hydration model are given in Table 4. These parameters can be divided into three groups, as the parameters relating to Portland cement hydration (B_{20}, C, k_{r20}, D_{e20}, β_1, β_2, $\frac{E}{R}$), the parameters relating to reactions of slag (B_{20SG},C_{SG}, k_{rSG20}, D_{eSG20}, β_{1SG}, β_{2SG}, $\frac{E_{SG}}{R}$), and the parameters relating to the pozzolanic reaction of fly ash (B_{20FA}, C_{FA}, k_{rFA20}, D_{eFA20}, β_{1FA}, β_{2FA}, $\frac{E_{FA}}{R}$).

The calibration process for these parameters is as follows:

First, based on the experimental results for adiabatic temperature increase in Portland cement, parameters relating to Portland cement hydration are calibrated. In this process, a predictor-corrector algorithm is adopted to confirm the values of the coefficients [31]. This algorithm proceeds in two steps: first, the prediction step calculates a rough approximation of the desired

Table 3
The mixing proportions of concrete.

	Water (kg/m^3)	Cement (kg/m^3)	Fly ash (kg/m^3)	Slag (kg/m^3)	Sand (kg/m^3)	Aggregate (kg/m^3)	Water-to- binder ratio	Water reducing agent (C×%)
OPC400	157	400	–	–	658	1129	0.392	0.25
OPC300	148	300	–	–	765	1129	0.493	0.25
OPC200	157	200	–	–	862	1089	0.785	0.25
MPC300	148	300	–	–	770	1129	0.493	0.25
OPC-paste	485	1620	–	–	–	–	0.3	–
SG400	157	240	–	160	645	1129	0.392	0.25
SG300	148	180	–	120	757	1129	0.493	0.25
SG200	157	120	–	80	854	1089	0.785	0.25
SG60	148	120	–	180	752	1131	0.493	0.75
SG70	147	90	–	210	755	1131	0.493	0.75
SG80	145	60	–	240	755	1131	0.483	0.75
SG40%-paste	477	954	–	636	–	–	0.3	–
FA400	157	320	80	–	639	1129	0.392	0.25
FA300	148	240	60	–	749	1129	0.493	0.25
FA200	157	160	40	–	852	1089	0.785	0.25
FA15[a]	147	255	45	–	823	1041	0.49	0.75
FA30[a]	147	210	90	–	806	1041	0.49	0.75
FA45[a]	147	165	135		789	1041	0.49	0.75
FA40%-paste	449	899	599	–	–	–	0.3	–
FA90%-paste	411	137	1233	–	–	–	0.3	–

[a] The cement employed in this mixing is moderate-heat Portland cement.

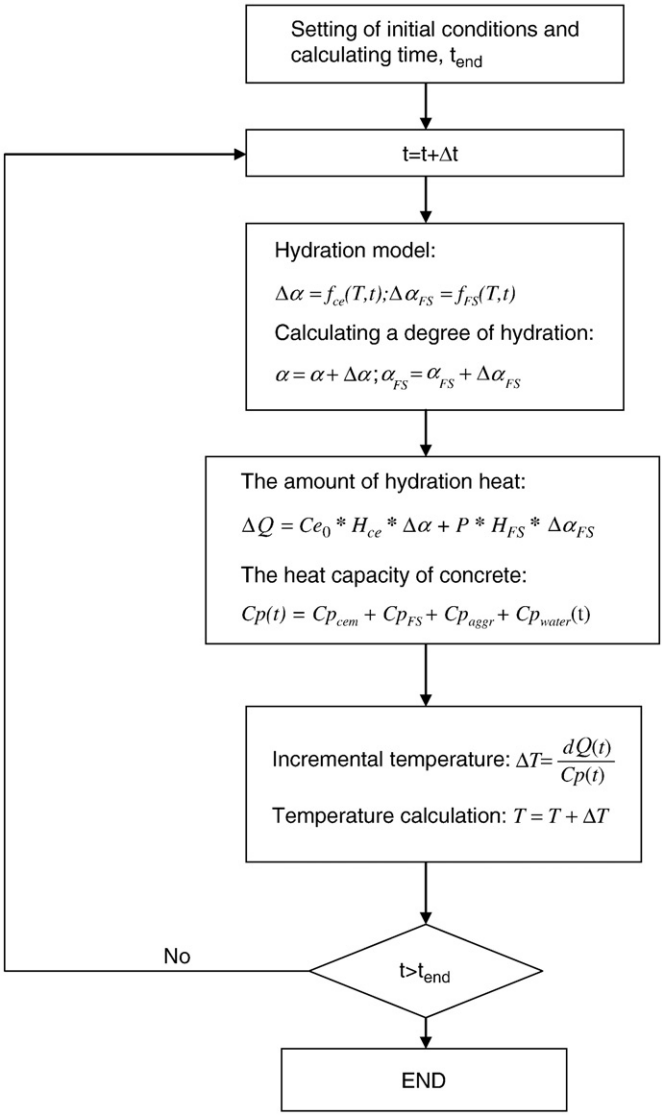

Fig. 2. The flow chart of numerical simulation process.

quantity; second, the corrector step refines the initial approximation by other means.

Second, in the case of slag-blended concrete, the heat evolution includes the contributions from both the cement hydration and the slag reaction. The contribution from the cement hydration can be evaluated with the parameters obtained in the first step. Based on the experimental results on the adiabatic temperature increase of slag-blended concrete and the predictor-corrector algorithm, the parameters relating to the slag reaction can be calibrated.

Third, in the case of fly ash blended concrete, the condition is similar to that of slag-blended concrete but the initial dormant period becomes prolonged due to the physical effect of the fly ash. For fly ash blended concrete, the parameter B_{20} is multiplied by a factor of 0.3, which means that the hydration rate of Portland cement in the initial dormant period is reduced and the initial dormant period is prolonged correspondingly.

Last, based on the parameters obtained in steps 1 to 3, multiple checks, including not only the early-age temperature test under adiabatic and semi-adiabatic conditions but also the evolution of chemically bound water, are carried out in the verification stage. The fit parameters for a material are not changed from one mix to the other.

Table 4
The coefficients of the hydration model.

B_{20}[a] (cm/h)	C (cm/(cm^4 h))	k_{r20}[a] (cm/h)	D_{e20}[a] (cm^2/h)	β_1 (K)	β_2 (K)	$\frac{E}{R}$ (K)
7.92×10^{-9}	1×10^{15}	7.84×10^{-6}	9.28×10^{-8}	1000	7500	5400
B_{20FA} (cm/h)	C_{FA} (cm/(cm^4 h))	k_{rFA20} (cm/h)	D_{eFA20} (cm^2/h)	β_{1FA} (K)	β_{2FA} (K)	$\frac{E_{FA}}{R}$ (K)
2.51×10^{-9}	1×10^{15}	1.71×10^{-6}	8.58×10^{-8}	1000	6000	4500
B_{20SG} (cm/h)	C_{SG} (cm/(cm^4 h))	k_{rSG20} (cm/h)	D_{eSG20} (cm^2/h)	β_{1SG} (K)	β_{2SG} (K)	$\frac{E_{SG}}{R}$ (K)
7.98×10^{-8}	1×10^{15}	9.80×10^{-6}	5.92×10^{-8}	1000	7000	5000

[a] For moderate-heat Portland cement, B_{20}, k_{r20}, and D_{e20} are 3.01×10^{-9}, 5.26×10^{-6}, and 1.48×10^{-8}, respectively.

The comparisons between the experimental results and the prediction results on the adiabatic temperature test are shown in Fig. 3 (OPC concrete), Fig. 4 (fly ash concrete), and Fig. 5 (slag concrete). The reduction in the adiabatic temperature rise at the completion of the reaction when the water-to-cement ratio is low was modeled. The comparison between the experimental and prediction results on chemically bound water is shown in Fig. 6. As shown in this figure, the prediction results generally agreed with the experimental results. It can be seen that in the case of the cement–fly ash paste compared with that of the control specimen, the amount of chemically bound water decreases with the replacement ratio of fly ash increasing (from Fig. 6-b to c, the replacement ratio of fly ash increases from 40% to 90%). On the other hand, the slag reactions are significantly affected by the amount of free water available for hydration. This distinction can be attributed to the difference in the hydration characteristics between fly ash and slag. Fly ash is a pozzolanic material, while slag is a truly hydraulic material, as explained in Section 3.1.

As shown in Figs. 3-e, 4-e, and 5-e, the modeling results generally agree with the experimental results. The correlation coefficients and the standard deviation between the modeled results and the experimental results for the adiabatic temperature rise test are approximately 0.99 and 3 °C respectively. However, for some cases, such as the fly ash blended concrete with a 10 °C initial temperature (Fig. 4-a), the slag concrete with a 30 °C initial temperature (Fig. 5-c), the slag concrete with extreme large slag replacements (for slag replacement ratio 80% in Fig. 5-d), and the fly ash blended concrete with different replacement ratios (Fig. 4-d), the modeling results show disagreements with the experimental results. These differences come from the following reasons.

For the fly ash blended concrete with a 10 °C initial temperature (Fig. 4-a), the difference between the prediction results and the experimental results mainly comes from the temperature dependence of the delaying effect and the decrease of the second peak in the heat generation rate when adding the retarder [12]. When the replacement ratio of fly ash or the amount of chemical admixtures is higher, the temperature dependence of the delaying effect and the decreasing of the second peak in the heat generation rate become significant.

For the slag concrete with a 30 °C initial temperature (Fig. 5-c), the difference between the prediction results and the experimental results mainly comes from the starting temperature of the test and the time for hydration (the casting time from mixing to the beginning of measurement). During this casting period, the blast furnace slag will react with gypsum and produce ettringite. The release heat from this reaction relates with the slag amount and the casting temperatures [12]. When other conditions are same, the more slag amount and the higher casting temperature, the more heat generate during

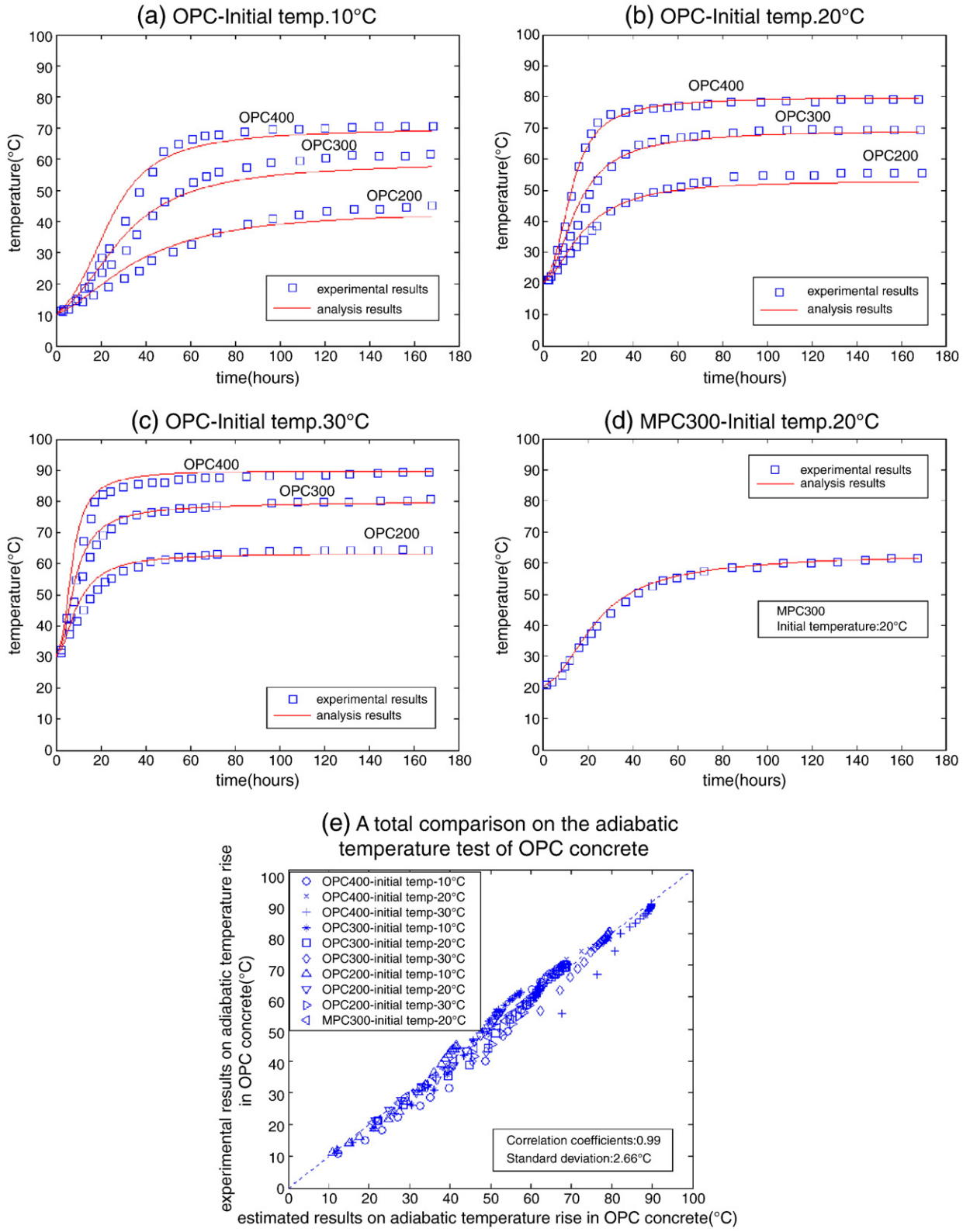

Fig. 3. The comparison between experimental results and prediction results on adiabatic temperature test of OPC concrete.

this period. In the current model, the heat generation from mixing to the beginning of measurement is not explicitly considered. So for SG400 with a 30 °C initial temperature, the analysis results are slightly higher than the experimental results.

For the slag concrete with extreme large slag replacements (for SG replacement ratio 80% in Fig. 5-d), the difference between prediction results and the experimental results mainly comes from the interlinked hydration pattern of slag with Portland cement [10]. In fact, the interlinked hydration pattern may be influenced by the phase concentration of pore solutions and pH level. For most of the practical cases of interest, i.e. when $Ca(OH)_2$ does not become a critical factor in the hydration reactions, the mutual interactions can be considered

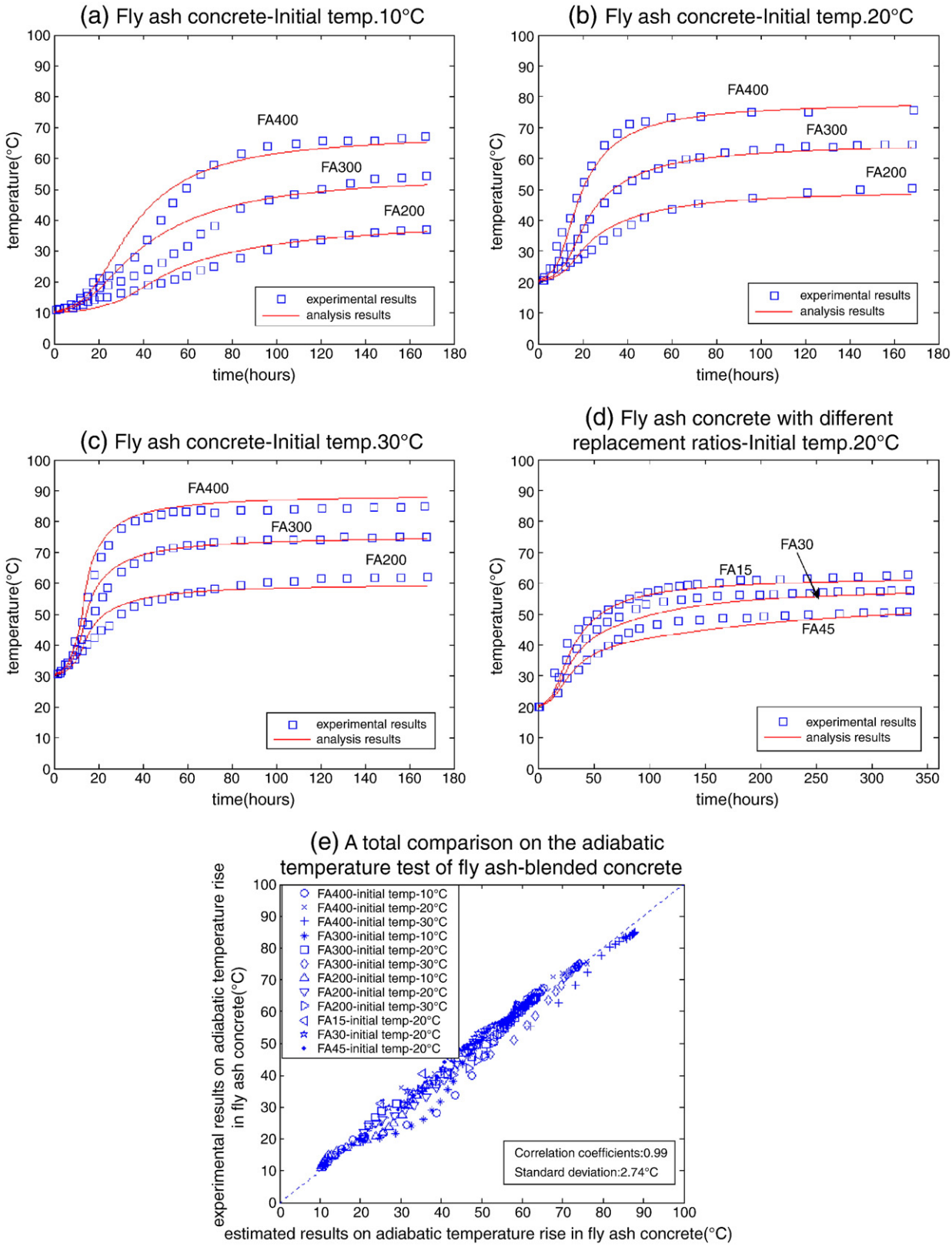

Fig. 4. The comparison between experimental results and prediction results on adiabatic temperature test of fly ash concrete.

through the amount of calcium hydroxide and capillary water left in the system, and the proposed model can give reasonable estimations [10,23].

For the fly ash blended concrete with different replacement ratios (Fig. 4-d), the disagreement mainly comes from the micro-filler effect by stagnated reaction binders (when the fly ash or slag reaction stagnates due to a shortage of $Ca(OH)_2$, the stagnated reacted fly ash particles or slag particles may have a micro-filler effect on the other reacting clinker materials). When the replacement ratio of fly ash or slag is higher, the micro-filler effect by stagnated reaction binders becomes significant

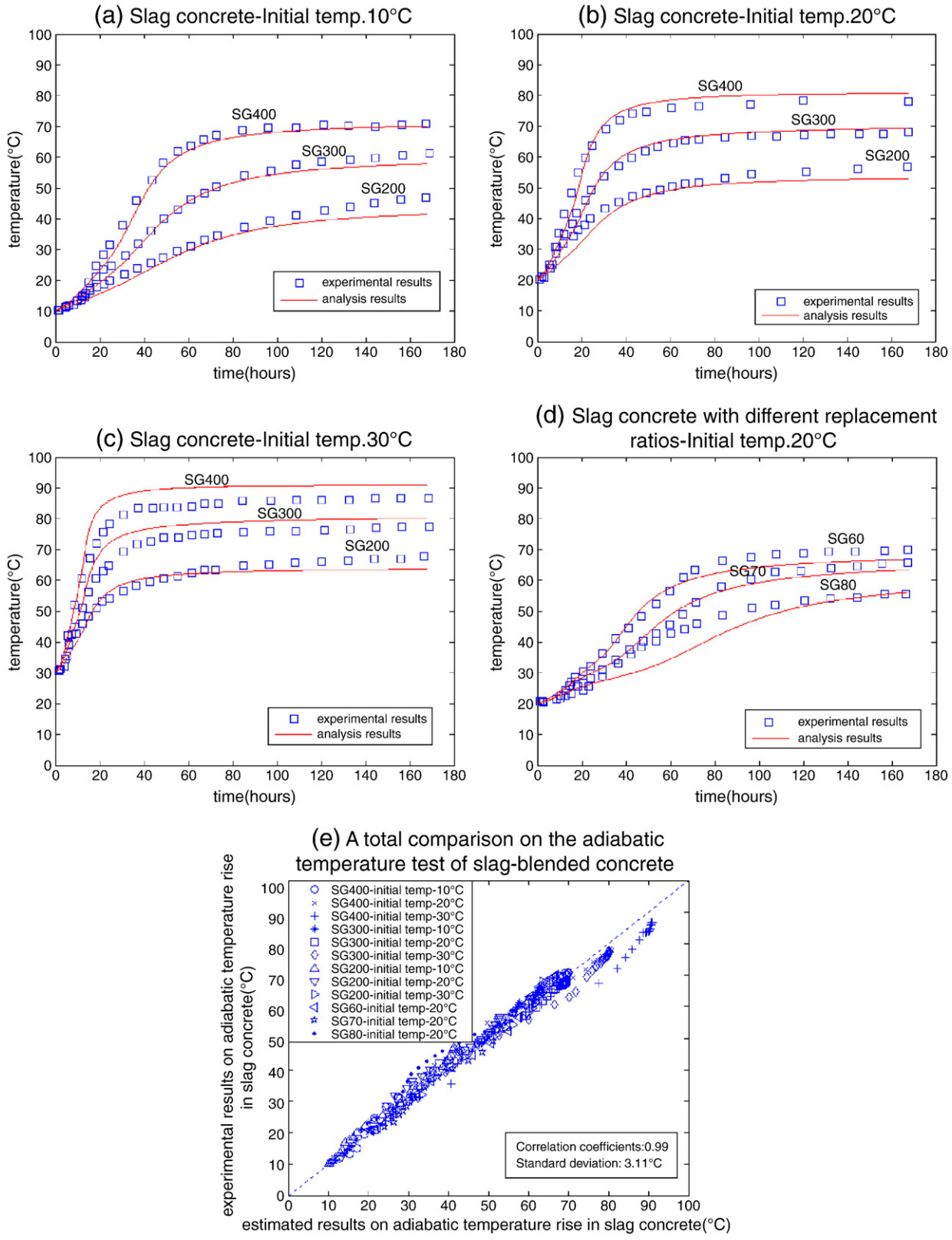

Fig. 5. The comparison between experimental results and prediction results on adiabatic temperature test of slag concrete.

[12]. In Fig. 4-d, when the replacement ratio of fly ash is 30% and 45%, the difference between analysis results and experimental results mainly comes from the ignorance of the micro-filler effect in my model. While in Ducom model, the micro-filler effect has been considered, so the results from updated new Ducom model show a better agreement with experimental results than my model [12].

The aforementioned factors affect the hydration of fly ash or slag-blended cement simultaneously with different weights. Depending on

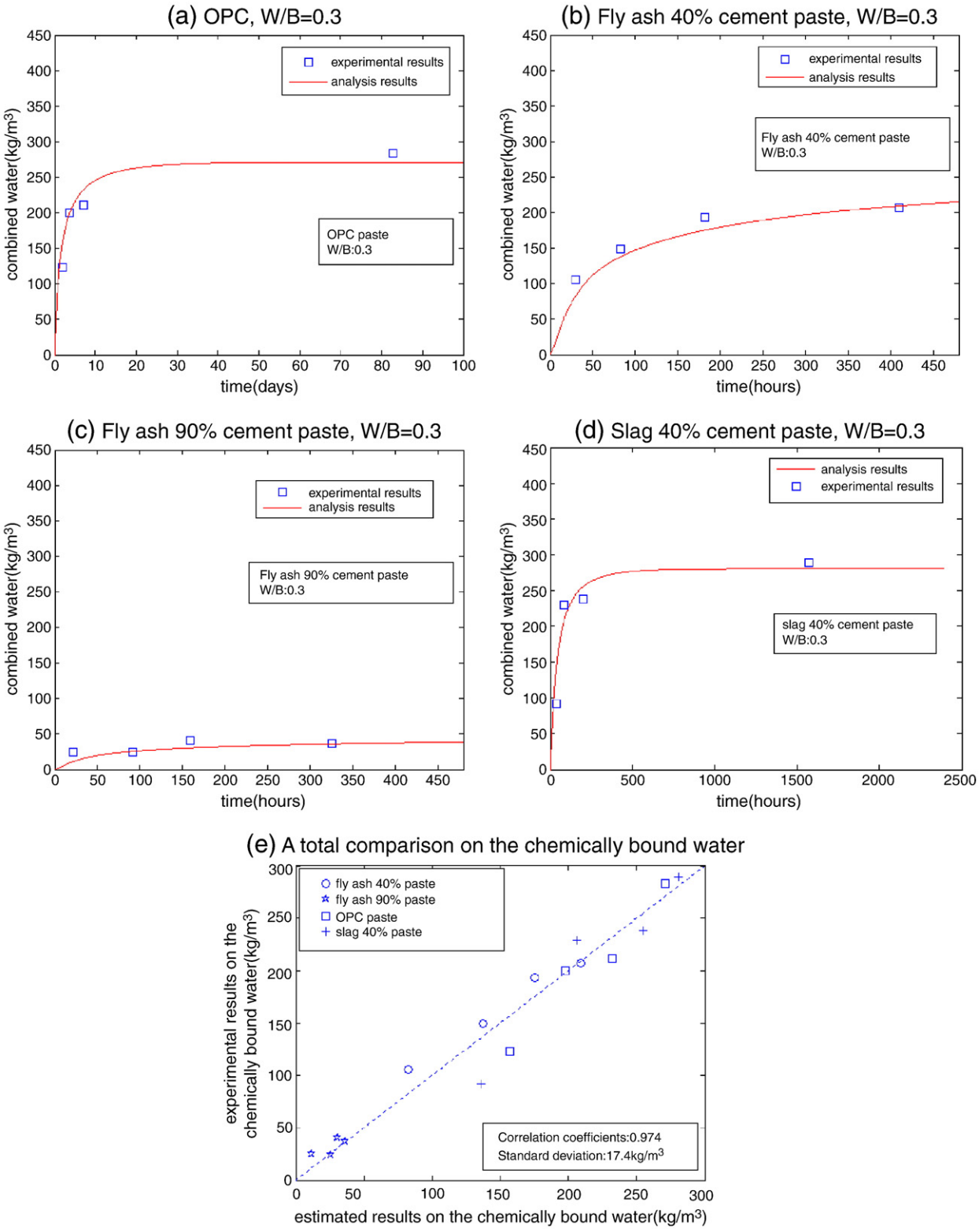

Fig. 6. The comparison between experimental results and prediction results on chemically bound water of OPC, fly ash and slag cement paste.

these variables, the model predicts the measured values with different degrees of accuracy. In addition, it should be noted that the influences of the chemical compositions of fly ash or slag, such as glass phase, SiO_2, and CaO contents, on the stoichiometries of the hydration reactions of fly ash and slag are not considered in this paper. The particle size distributions of fly ash and slag are simplified to be monosize so that when the Blaine surface represents substantial changes, the coefficients in the reaction of mineral admixtures may be changed correspondingly.

At the current stage, the model is limited in that some variables are not accounted for. The model will be subject to further improvement in the future.

5. Comparison to other hydration models

In the past years, a few models, for example Hymostruc model [42–48], Schutter's model [14,15,49–52], CEMHYD3D model [53–62], Papadakis' chemical-based steady-state model [18–22] and Ducom model [10–12], have been built to evaluate the development of properties of Portland cement concrete and blended cement concrete which incorporates mineral admixtures, such as limestone filler, silica fume, slag and fly ash.

K. van Breugel [42–48] built the Hymostruc model which can simulate the development of properties of Portland cement-based materials, e.g. the development of hydration and microstructure [42–44,47], the thermodynamic equilibrium and the volume changes of hardening cement paste [45], and the effect of geometrical changes of the microstructure on the creep behavior of hardening concrete [46]. The hydration curves were predicted as a function of the particle size distribution, chemical composition of cement, the water-to-cement ratio and the actual reaction temperature. The old Hymostruc model [42–47] is valid only for Portland cement. Recently, based on the hydration chemistry, the stoichiometry and the hydration kinetics, Ye Guang [48] made an improvement on Hymostruc model to consider the effect of limestone filler. So at the current version, the Hymostruc is valid for Portland cement and limestone filler blended cement. The effect of other reactive mineral admixtures, such as silica fume, slag and fly ash, is not considered in the current Hymostruc model.

Schutter [14,15,49–52] proposed a kinetic hydration model which is valid for Portland cement, high filler blended cement and blast furnace slag cement. In Schutter's model, the heat evolution of blast furnace slag cement is obtained by the superposition of the heat productions of the Portland reaction (P reaction) and the slag reaction (S reaction) [14,49]. The evolution of mechanical properties in early-age concrete is described using functions of the degree of hydration [15]. However, Schutter's model does not explicitly consider the interactions between the cement hydration and the reaction of mineral admixtures, such as the producing of calcium hydroxide by cement hydration and the consumption by slag reaction. The generalization of the reaction parameters depending on the actual slag replacement ratios is not yet possible [49]. Contrastively, the proposed model in this paper is valid for Portland cement, silica fume cement, slag cement and fly ash cement. The mutual interactions between cement hydration and the reaction of slag are considered based on the amount of capillary water and the amount of calcium hydroxide left in the system. The fit parameters for a material are not changed from one mix to the other.

Edward J. Garboczi, Dale P. Bentz and co-researchers [53–62] built a three-dimensional cement hydration and microstructure development program, CEMHYD3D. CEMHYD3D model can simulate the development of properties of cement-based materials, such as the hydration of limestone filler blended cement [53,54], the adiabatic temperature rising of Portland cement concrete and silica fume blended concrete [55], and the diffusivity of chloride ions in silica fume blended cement paste [56,57]. CEMHYD3D model has preliminary incorporated the reaction of fly ash [58] and slag [59–62]. However, compared with silica fume, the chemical reactions involved in the fly ash or slag-blended cement are much more complex, so Bentz [58–62] stated that to achieve a good simulation result, more effort should be done on the reaction kinetic constant and activation energy of the reaction of fly ash or slag. The induction period of slag or fly ash blended concrete is not explicitly considered in CEMHYD3D model, which limits its application in predicting the properties of early-age concrete [55,58,62]. Contrastively, in this paper, based on the experimental results on adiabatic temperature rise, the reaction parameters of fly ash cement and slag cement are obtained. The model is further verified through the experimental results on chemically bound water. The influence of fly ash on the induction period is considered in this paper, and the temperature history and temperature distribution of blended cement concrete are predicted.

Based on the experimental results of reaction stoichiometries among silica fume or fly ash, chemical bound water and calcium hydroxide, Papadakis and co-researchers [18–22] proposed a simplified scheme that describes the activity of silica fume and fly ash in terms of chemical reactions. Furthermore, the effect of supplementary cementing materials on the concrete resistance against carbonation and chloride ingress is evaluated through the stoichiometry of chemical reactions and mathematical models. But, it should be noticed that Papadakis' chemical-based steady-state model is not a kinetic model. The kinetic of pozzolanic reactions, for example the calcium hydroxide that is produced by cement hydration and consumed by pozzolanic reaction, were not reflected in his model. Papadakis' model can estimate only the final chemical and volumetric composition of a silica fume or fly ash blended concrete after completing hydration and pozzolanic reactions and establishing a steady state. Contrastively, in our previous research [63–65], by combining Papadakis' chemical-based steady-state model with kinetics involved in the reactions of fly ash or silica fume, kinetic reaction models of the silica fume or fly ash blended cement have been built. The influence of mineral compositions of fly ash or silica fume on reaction stoichiometry is considered [63–65]. The evolution of chemical and volumetric composition of silica fume–cement blends or fly ash–cement blended is predicted as a function of curing age [63–65].

Maekawa and co-researchers [10–12] proposed an integrated program, Ducom (durability concrete model), which can be employed to evaluate both the early-age properties of hardening concrete (such as the cement heat hydration and thermal conduction, pore structure formation and moisture equilibrium) and durability of concrete (for example chloride ion transport, carbonation, corrosion of steel rebar and calcium ion leaching). The old Ducom model [10] can be used to evaluate the temperature history of slag or fly ash blended concrete. On the other hand, in the new updated Ducom model [12], the effect of limestone powder and the reaction of silica fume are incorporated. However, due to the complexity of the chemical reactions in the binary cement, Ducom model did not consider too much on the chemical aspects of the hydration of binary cement. The influence of mineral compositions of fly ash or silica fume on reaction stoichiometry is not considered in Ducom model [12]. The evolution of chemical and volumetric composition of silica fume–cement blends or fly ash–cement blends cannot be evaluated [12]. In our previous study, this point has been solved [63–65].

Summarily, Hymostruc model [42–48], Schutter's model [14,15,49–52], CEMHYD3D model [53–62], Papadakis' chemical-based steady-state model [18–22] and Ducom model [10–12] are globally advanced in the modeling of the properties of cement-based materials. But, as far as the modeling of hydration of fly ash or slag is concerned, the aforementioned models show some disadvantages. The proposed model in this paper and our previous study [63–65] overcome these disadvantages. On the other hand, using the calibration process proposed in this paper, it is convenient for other researchers to use our hydration model. This model also can be integrated into other commercial software as a module for predicting the properties of hardening blended concrete.

As proposed by Breugel [66] and Bentz [67], knowledge of the microstructures of cement-based materials is necessary to determine their mechanical and physical properties, as well as their transport properties and related durability. Integrated kinetic hydration models consider the formation of the microstructure and its effect on the rate of hydration. Those models are thought to be promising for computational research on cement-based systems. Furthermore, a multi-scale model of concrete performance can be built to integrate material science and structural mechanics. Macroscopic characters of concrete composites are dependent upon micro-pore structures and thermodynamic states associated with durability. In turn, chemo-physical states of substances in nano-pores are strongly associated with structural mechanics and damage induced by loads and weather actions. The chemo-physics and mechanical modeling of concrete on different geometric scales can be used in quantitative assessments of

structural concrete performance and may help engineers in charge of design, planning and policymaking [12].

6. Conclusions

1. In this paper, a kinetic model is proposed to describe the hydration process of concrete containing fly ash or slag. By considering the production of calcium hydroxide in cement hydration and its consumption during the reaction of mineral admixtures, the reaction of fly ash or slag is separated from the cement hydration. The equation for the reaction of mineral admixtures can be derived from that of cement hydration by considering both the similarities and the differences between the two reactions. Similar to the hydration reaction of cement, the reaction of mineral admixtures is divided into three processes: the initial dormant period, a phase-boundary reaction process, and a diffusion process. The proposed model considers the dependence of the reaction of mineral admixtures on the mass of calcium hydroxide.
2. The heat release rate is determined by the contribution of both cement hydration and reactions of mineral admixtures. Furthermore, the temperature rise is evaluated based on the degrees of hydration of the cement and the mineral admixtures. The simulation results agree well with the experimental results with regard to the adiabatic and quasi-adiabatic temperature rise history and chemically bound water.

Acknowledgements

The authors are grateful to Professor Koichi Maekawa and Professor Toshiaru Kishi in the University of Tokyo for the kind assistance on experimental results.

This study was supported by the Engineering Research Center designated by the Ministry of Education & Science Technology, and Sustainable Building Research Center, Hanyang University (R11-2005-056-04003). This research was supported by a grant (06-CIT-A02: Standardization Research for Construction Materials) from Construction Infrastructure Technology Program funded by Ministry of Land, Transport and Marine Affairs.

References

[1] P. Kumar Metha, Paulo J.M. Monteiro, Concrete, Microstructure, Properties and Materials, McGraw-Hill, New York, 2006.
[2] H.F.W. Taylor, Cement Chemistry, Thomas Telford, London, 1997.
[3] F. Tomosawa, T. Noguchi, C. Hyeon, Simulation model for temperature rise and evolution of thermal stress in concrete based on kinetic hydration model of cement, in: S. Chandra (Ed.), Proceedings of Tenth International Congress Chemistry of Cement. Gothenburg, Sweden, vol. 4, 1997, pp. 72–75.
[4] Ki-Bong Park, Prediction of cracking in high strength concrete using a hydration model, PhD dissertation, The University of Tokyo, 2001.
[5] Ki-Bong Park, Nam-Yong Jee, In-Seok Yoon, Han-Seung Lee, Prediction of temperature distribution in high-strength concrete using hydration model, ACI Mater J 105 (2008) 180–186.
[6] S. Swaddiwudhipong, D. Shen, M.H. Zhang, Simulation of the exothermic hydration process of Portland cement, Adv Cem Res 14 (2002) 61–69.
[7] Toshiharu Kishi, Koichi Maekawa, Multi-component model for hydration heating of Portland cement, Concrete library of JSCE 28 (1996) 97–115.
[8] L.J. Parrot, D.C. KILLOH, Prediction of cement hydration in the chemistry and chemically-related properties of cement, British Ceramic proceedings 35 (1984) 41–53.
[9] S. Swaddiwudhipong, H. Wu, M.H. Zhang, Numerical simulation of temperature rise of high strength concrete incorporating silica fume and superplasticizer, Adv Cem Res 15 (2003) 161–169.
[10] Koichi Maekawa, Rajesh Chaube, Toshiharu Kishi, Modeling of Concrete Performance: Hydration, Microstructure Formation and Mass Transport, ROUTLEDGE, London, 1998.
[11] Koichi Maekawa, Tetsuya Ishida, Modeling of structural performances under coupled environmental and weather actions, Mater Struc 35 (2002) 591–602.
[12] Koichi Maekawa, Tetsuya Ishida, Toshiharu Kishi, Multi-scale Modeling of Structural Concrete, Taylor & Francis, London, 2009.
[13] Satoshi Tanaka, Kazuhisa Inoue, Yoshihide Shioyama, Rokuro Tomita, Methods of estimating heat of hydration and temperature rise in blast furnace slag blended cement, ACI Mater J 92 (1995) 429–436.
[14] G. De Schutter, L. Taerwe, General hydration model for Portland cement and blast furnace slag cement, Cem Concr Res 25 (1995) 593–604.
[15] G. De Schutter, L. Taerve, Degree of hydration-based description of mechanical properties of early age concrete, Mater Struc 29 (1996) 335–344.
[16] Ippei Maruyama, Numerical model for hydration of Portland cement, Proceedings of the International Conference of Civil and Environmental Engineering, Hiroshima, Japan, 2003, pp. 53–62.
[17] P. Navi, C. Pignat, Simulation of cement hydration and the connectivity of the capillary pore space, Adv Cem Based Mater 4 (1996) 58–67.
[18] Vagelis G. Papadakis, Experimental investigation and theoretical modeling of silica fume activity in concrete, Cem Concr Res 29 (1999) 79–86.
[19] Vagelis G. Papadakis, S. Tsimas, Effect of supplementary cementing materials on concrete resistance against carbonation and chloride ingress, Cem Concr Res 30 (2000) 291–299.
[20] Vagelis G. Papadakis, Effect of fly ash on Portland cement systems, Part I: low-calcium fly ash, Cem Concr Res 29 (1999) 1727–1736.
[21] Vagelis G. Papadakis, Effect of fly ash on Portland cement systems, Part II: high calcium fly ash, Cem Concr Res 30 (2000) 1647–1654.
[22] V.G. Papadakis, C.G. Vayenas, M.N. Fardis, Physical and chemical characteristics affecting the durability of concrete, ACI Mater J 88 (1991) 186–196.
[23] Tatsuhiko Saeki, Paulo J.M. Monteiro, A model to predict the amount of calcium hydroxide in concrete containing mineral admixture, Cem Concr Res 35 (2005) 1914–1921.
[24] Ivindra Pane, Will Hansen, Investigation of blended cement hydration by isothermal calorimetry and thermal analysis, Cem Concr Res 35 (2005) 1155–1164.
[25] K. Takemoto, H. Uchikawa, Hydration of pozzolanic cement, Proceeding of the 7th International Congress on Chemistry of Cement, Paris, 1980.
[26] Wei Chen, H.J. Brouwers, Z.H. Shui, Three-dimensional computer modeling of slag cement hydration, J Mater Sci 42 (2007) 9595–9610.
[27] A. Fernandez-Jimenez, F. Puertas, A. Arteaga, Determination of kinetic equations of alkaline activation of blast furnace slag by means of calorimetric data, J Thermal Anal 52 (1998) 945–955.
[28] J.I. Escalante, L.Y. Gomez, K.K. Johal, G. Mendoza, H. Mancha, J. Mendez, Reactivity of blast furnace slag in Portland cement blends hydrated under different conditions, Cem Concr Res 31 (2001) 1403–1409.
[29] J.I. Escalante-Garera, J.H. Sharp, The microstructure and mechanical properties of blended cements hydrating at various temperatures, Cem Concr Res 31 (2001) 695–702.
[30] Ippei Maruyama, Masahiro Suzuki, Ryoichi Sato, Prediction of temperature in ultra high-strength concrete based on temperature dependent hydration model, in: Henry G. Russell (Ed.), ACI SP-228, Proc. of 7th Int. Symp on High Performance Concrete, 2005, pp. 1175–1186.
[31] C. Hyun, Prediction of thermal stress of high strength concrete and massive concrete, PhD dissertation, The University of Tokyo, 1995.
[32] Yasuo Arai, Chemistry of Cement Materials, Dai-Nippon Tosho Publishing Co. Ltd, Tokyo, 1993.
[33] Walter A. Gutteridge, John A. Dalziel, Filler cement: the effect of the secondary component on the hydration of Portland cement: Part I. A fine non-hydraulic filler, Cem Concr Res 20 (1990) 778–782.
[34] Walter A. Gutteridge, John A. Dalziel, Filler cement: the effect of the secondary component on the hydration of Portland cement: Part 2: fine hydraulic binders, Cem Concr Res 20 (1990) 853–861.
[35] Philippe Lawrence, Martin Cyr, Erick Ringot, Mineral admixtures in mortars: effect of inert materials on short-term hydration, Cem Concr Res 33 (2003) 1939–1947.
[36] Martin Cyr, Philippe Lawrence, Erick Ringot, Mineral admixtures in mortars: quantification of the physical effects of inert materials on short-term hydration, Cem Concr Res 35 (2005) 719–730.
[37] Philippe Lawrence, Martin Cyr, Erick Ringot, Mineral admixtures in mortars effect of type, amount and fineness of fine constituents on compressive strength, Cem Concr Res 35 (2005) 1092–1105.
[38] Martin Cyr, Philippe Lawrence, Erick Ringot, Efficiency of mineral admixtures in mortars: quantification of the physical and chemical effects of fine admixtures in relation with compressive strength, Cem Concr Res 36 (2006) 264–277.
[39] K.A. Paine, L. Zheng, R.K. Dhir, Experimental study and modeling of heat evolution of blended cement, Adv Cem Res 17 (2005) 121–132.
[40] C. Cang, C. Dilger, Prediction of temperature distribution in hardening concrete, in: Springenschmid (Ed.), Thermal Crack in Concrete at Early Ages, E&FN SPON, London, UK, 1994, pp. 21–28.
[41] Daryl L. Logan, A First Course in the Finite Element Method, Third editionBrooks/Cole Thomson learning, United States, 2002.
[42] K. van Breugel, Numerical simulation of hydration and microstructural development in hardening cement-based materials (I) Theory, Cem Concr Res 25 (1995) 319–331.
[43] K. van Breugel, Numerical simulation of hydration and microstructural development in hardening cement-based materials (II) Applications, Cem Concr Res 25 (1995) 522–530.
[44] Antonio Princigallo, Pietro Lura, Klaas van Breugel, Giovanni Levita, Early development of properties in a cement paste: a numerical and experimental study, Cem Concr Res 33 (2003) 1013–1020.
[45] E.A.B. Koenders, K. van Breugel, Numerical modelling of autogenous shrinkage of hardening cement paste, Cem Concr Res 27 (1997) 1489–1499.
[46] S.J. Lokhorst, K. van Breugel, Simulation of the effect of geometrical changes of the microstructure on the deformational behaviour of hardening concrete, Cem Concr Res 27 (1997) 1465–1479.
[47] G. Ye, K. van Breugel, A.L.A. Fraaij, Three-dimensional microstructure analysis of numerically simulated cementitious materials, Cem Concr Res 30 (2003) 215–222.

[48] G. Ye, X. Liu, A.M. Poppe, G. De Schutter, K. van Breugel, Numerical simulation of the hydration process and the development of microstructure of self-compacting cement paste containing limestone as filler, Mater Struc 40 (2007) 865–875.
[49] Geert De Schutter, Hydration and temperature development of concrete made with blast-furnace slag cement, Cem Concr Res 29 (1999) 143–149.
[50] Anne-Mieke Poppe, Geert De Schutter, Cement hydration in the presence of high filler contents, Cem Concr Res 35 (2005) 2290–2299.
[51] G.D. Schutter, Finite element simulation of thermal cracking in massive hardening concrete elements using degree of hydration based material laws, Comp Struc 80 (2002) 2035–2042.
[52] G. De Schutter, L. Taerwe, towards a more fundamental non-linear basic creep model for early-age concrete, Mag Concr Res 49 (1997) 195–200.
[53] D.P. Bentz, Modeling the influence of limestone filler on cement hydration using CEMHYD3D, Cem Concr Comp 28 (2006) 124–129.
[54] Dale P. Bentz, Influence of water-to-cement ratio on hydration kinetics: simple models based on spatial considerations, Cem Concr Res 36 (2006) 238–244.
[55] D.P. Bentz, V. Waller, F. de Larrard, Prediction of adiabatic temperature rise in conventional and high-performance concretes using a 3-D microstructural model, Cem Concr Res 28 (1998) 285–297.
[56] D.P. Bentz, O.M. Jensen, A.M. Coats, F.P. Glasser, Influence of silica fume on diffusivity in cement-based materials: I. Experimental and computer modeling studies on cement pastes, Cem Concr Res 30 (2000) 953–962.
[57] D.P. Bentz, Influence of silica fume on diffusivity in cement-based materials: II. Multi-scale modeling of concrete diffusivity, Cem Concr Res 30 (2000) 1121–1129.
[58] Dale P. Bentz, Sebastien Remond, Incorporation of Fly Ash into a 3-D Cement Hydration Microstructure Model, NISTIR 6050, 1997.
[59] John M. Richardson, Joseph J. Biernacki, Paul E. Stutzman, Dale P. Bentz, Stoichiometry of slag hydration with calcium hydroxide, J Am Ceram 85 (2002) 947–953.
[60] J.J. Biernacki, J.M. Richardson, P.E. Stutzman, D.P. Bentz, Kinetics of slag hydration in the presence of calcium hydroxide, J Am Ceram 85 (2002) 2261–2267.
[61] D.P. Bentz, modeling cement microstructure: pixels, particles and property prediction, Mater Struc 32 (1999) 187–195.
[62] D.P. Bentz, CEMHYD3D: A Three-Dimensional Cement Hydration and Microstructure Development Modelling Package. Versions 3.0 and 2.0, NISTIR 7232, June 2005.
[63] Xiao-Yong Wang, Han-Seung Lee, A model predicting carbonation depth of concrete containing silica fume, Mater Struc 42 (2009) 691–704.
[64] Xiao-Yong Wang, Han-Seung Lee, A model for predicting the carbonation depth of concrete containing low-calcium fly ash, Constr Buil Mater 23 (2009) 725–733.
[65] Xiao-Yong Wang, Han-Seung Lee, Ki-Bong Park, Simulation of low-calcium fly ash blended cement hydration, ACI Mater J 106 (2009) 167–175.
[66] K. van Breugel, Modeling of cement-based systems—the alchemy of cement chemistry, Cem Concr Res 34 (2004) 1661–1668.
[67] Dale P. Bentz, A three-dimensional cement hydration and microstructure program. I. Hydration rate, heat of hydration, and chemical shrinkage, NIST internal report 5756 (1995).